

Deep Portfolio Optimization via Distributional Prediction of Residual Factors

Kentaro Imajo,¹ Kentaro Minami,¹ Katsuya Ito,¹ Kei Nakagawa,²

¹ Preferred Networks, Inc.

² Nomura Asset Management Co., Ltd.

{imos, minami, katsuya@preferred.jp, k-nakagawa@nomura-am.co.jp}

Abstract

Recent developments in deep learning techniques have motivated intensive research in machine learning-aided stock trading strategies. However, since the financial market has a highly non-stationary nature hindering the application of typical data-hungry machine learning methods, leveraging financial inductive biases is important to ensure better sample efficiency and robustness. In this study, we propose a novel method of constructing a portfolio based on predicting the distribution of a financial quantity called residual factors, which is known to be generally useful for hedging the risk exposure to common market factors. The key technical ingredients are twofold. First, we introduce a computationally efficient extraction method for the residual information, which can be easily combined with various prediction algorithms. Second, we propose a novel neural network architecture that allows us to incorporate widely acknowledged financial inductive biases such as amplitude invariance and time-scale invariance. We demonstrate the efficacy of our method on U.S. and Japanese stock market data. Through ablation experiments, we also verify that each individual technique contributes to improving the performance of trading strategies. We anticipate our techniques may have wide applications in various financial problems.

1 Introduction

Developing a profitable trading strategy is a central problem in the financial industry. Over the past decade, machine learning and deep learning techniques have driven significant advances across many application areas (Devlin et al. 2019; Graves, Mohamed, and Hinton 2013), which inspired investors and financial institutions to develop machine learning-aided trading strategies (Wang et al. 2019; Choudhry and Garg 2008; Shah 2007). However, it is believed that forecasting the nature of financial time series is essentially a difficult task (Krauss, Do, and Huck 2017). In particular, the well-known *efficient market hypothesis* (Malkiel and Fama 1970) claims that no single trading strategy could be permanently profitable because the dynamics of the market changes quickly. At this point, the financial market is significantly different from stationary environments typically assumed by most machine learning/deep learning methods.

Copyright © 2021, Association for the Advancement of Artificial Intelligence (www.aaai.org). All rights reserved.

Generally speaking, a good way for deep learning methods to adapt quickly to the given environment is to introduce a network architecture that reflects a good inductive bias for the environment. The most prominent examples for such architectures include convolutional neural networks (CNNs) (Krizhevsky, Sutskever, and Hinton 2012) for image data and long short-term memories (LSTMs) (Hochreiter and Schmidhuber 1997) for general time series data. Therefore, a natural question to ask is what architecture is effective for processing financial time series.

In finance, researchers have proposed various trading strategies and empirically studied their effectiveness. Hence, it is reasonable to seek architectures inspired by empirical findings in financial studies. In particular, we consider the following three features in the stock market.

1.1 Hedging exposures to common market factors

Many empirical studies on stock returns are described in terms of *factor models* (e.g., (Fama and French 1992, 2015)). These factor models express the return of a certain stock i at time t as a linear combination of K factors plus a residual term:

$$r_{i,t} = \sum_{k=1}^K \beta_i^{(k)} f_t^{(k)} + \epsilon_{i,t}. \quad (1)$$

Here, $f_t^{(1)}, \dots, f_t^{(K)}$ are the common factors shared by multiple stocks $i \in \{1, \dots, S\}$, and the residual factor $\epsilon_{i,t}$ is specific to each individual stock i . Therefore, the common factors correspond to the dynamics of the entire stock market or industries, whereas the residual factors convey some firm-specific information.

In general, if the return of an asset has a strong correlation to the market factors, the asset exhibits a large exposure to the risk of the market. For example, it is known that a classical strategy based on the *momentum* phenomenon (Jegadeesh and Titman 1993) is correlated to the Fama-French factors (Fama and French 1992, 2015), which exhibited negative returns around the credit crisis of 2008 (Calomiris, Love, and Peria 2010; Szado 2009). On the other hand, researchers found that trading strategies based only on the residual factors can be robustly profitable because such strategies can hedge out the time-varying risk exposure to the market factor (Blitz, Huij, and Martens 2011; Blitz et al.

2013). Therefore, to develop trading strategies that are robust to structural changes in the market, it is reasonable to consider strategies based on residual factors.

A natural way to remove the market effect and extract the residual factors is to leverage linear decomposition methods such as principal component analysis (PCA) and factor analysis (FA). In the context of training deep learning-based strategies, it is expected to be difficult to learn such decomposition structures only from the observed data. One possible reason is that the learned strategies can be biased toward using information about market factors because the effect of market factors are dominant in many stocks (Pasini 2017). Hence, in order to utilize the residual factors, it is reasonable to implement a decomposition-like structure explicitly within the architecture.

1.2 Designing architectures for scale invariant time series

When we address a certain prediction task using a neural network-based approach, an effective choice of neural network architecture typically hinges on *patterns* or *invariances* in the data. For example, CNNs (LeCun et al. 1999) take into account the shift-invariant structure that commonly appears in image-like data. From this perspective, it is important to find invariant structures that are useful for processing financial time series.

As candidates of such structures, there are two types of invariances known in financial literature. First, it is known that a phenomenon called volatility clustering is commonly observed in financial time series (Lux and Marchesi 2000), which suggests an invariance structure of a sequence with respect to its volatility (i.e., amplitude). Second, there is a hypothesis that sequences of stock prices have a certain time-scale invariance property known as the *fractal structure* (Peters 1994). We hypothesize that incorporating such invariances into the network architecture is effective at accelerating learning from financial time series data.

1.3 Constructing portfolios via distributional prediction

Another important problem is how to convert a given prediction of the returns into an actual trading strategy. In finance, there are several well-known trading strategies. To name a few, the momentum phenomenon (Jegadeesh and Titman 1993) suggests a strategy that bets the current market trend, while the mean reversion (Poterba and Summers 1988) suggests another strategy that assumes that the stock returns moves toward the opposite side of the current direction. However, as suggested by the construction, the momentum and the reversal strategies are negatively correlated to each other, and it is generally unclear which strategy is effective for a particular market. On the other hand, modern portfolio theory (Markowitz 1952) provides a framework to determine a portfolio from distributional properties of asset prices (typically means and variances of returns). The resulting portfolio is unique in the sense that it has an optimal trade-off of returns and risks under some predefined conditions. From this perspective, distributional prediction

of returns can be useful to construct trading strategies that can automatically adapt to the market.

1.4 Summary of contributions

- We propose a novel method to extract residual information, which we call the *spectral residuals*. The spectral residuals can be calculated much faster than the classical factor analysis-based method without losing the ability to hedge out exposure to the market factors. Moreover, the spectral residuals can easily be combined with any prediction algorithms.
- We propose a new system for distributional prediction of stock prices based on deep neural networks. Our system involves two novel neural network architectures inspired by well-known invariance hypotheses on financial time series. Predicting the distributional information of returns allows us to utilize the optimal portfolio criteria offered by modern portfolio theory.
- We demonstrate the effectiveness of our proposed methods on real market data.

In the supplementary material, we also include appendices which contain detailed mathematical formulations and experimental settings, theoretical analysis, and additional experiments.

2 Preliminaries

2.1 Problem setting

Our problem is to construct a time-dependent portfolio based on sequential observations of stock prices. Suppose that there are S stocks indexed by symbol i . The observations are given as a discrete time series of stock prices $\mathbf{p}^{(i)} = (p_1^{(i)}, p_2^{(i)}, \dots, p_t^{(i)}, \dots)$. Here, $p_t^{(i)}$ is the price of stock i at time t . We mainly consider the *return* of stocks instead of their raw prices. The return of stock i at time t is defined as $r_t^{(i)} = p_{t+1}^{(i)} / p_t^{(i)} - 1$.

A *portfolio* is a (time-dependent) vector of weights over the stocks $\mathbf{b}_t = (b_t^{(1)}, \dots, b_t^{(i)}, \dots, b_t^{(S)})$, where $b_t^{(i)}$ is the volume of the investment on stock i at time t satisfying $\sum_{i=1}^S |b_t^{(i)}| = 1$. A portfolio \mathbf{b}_t is understood as a particular trading strategy, that is, $b_t^{(i)} > 0$ implies that the investor takes a long position on stock i with amount $|b_t^{(i)}|$ at time t , and $b_t^{(i)} < 0$ means a short position on the stock. Given a portfolio \mathbf{b}_t , its overall return R_t at time t is given as $R_t := \sum_{i=1}^S b_t^{(i)} r_t^{(i)}$. Then, given the past observations of individual stock returns, our task is to determine the value of \mathbf{b}_t that optimizes the future returns.

An important class of portfolios is the *zero-investment portfolio* defined as follows.

Definition 1 (Zero-Investment Portfolio). A zero-investment portfolio is a portfolio whose buying position and selling position are evenly balanced, i.e., $\sum_{i=1}^S b_t^{(i)} = 0$.

In this paper, we restrict our attention to trading strategies that output zero-investment portfolio. This assumption is sensible because a zero-investment portfolio requires no

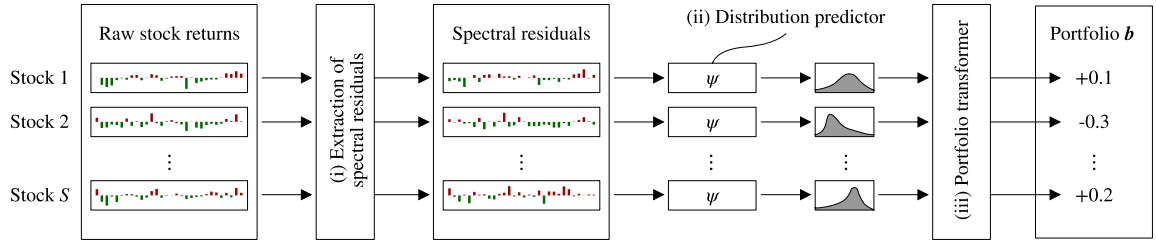


Figure 1: Overview of the proposed system. Our system consists of three parts: (i) the extraction layer of residual factors (ii) a neural network-based distribution predictor and (iii) transformation to the optimal portfolio.

equity and thus encourages a fair comparison between different strategies.

In practice, there can be delays between the observations of the returns and the actual execution of the trading. To account for this delay, we also adopt the delay parameter d in our experiments. When we trade with a d -day delay, the overall return should be $R_t := R_t^d = \sum_{i=1}^S b_t^{(i)} r_{t+d}^{(i)}$.

2.2 Concepts of portfolio optimization

According to modern portfolio theory (Markowitz 1952), investors construct portfolios to maximize expected return under a specified level of acceptable risk. The standard deviation is commonly used to quantify the risk or variability of investment outcomes, which measures the degree to which a stock’s annual return deviates from its long-term historical average (Kintzel 2007).

The Sharpe ratio (Sharpe 1994) is one of the most referenced risk/return measures in finance. It is the average return earned in excess of the risk-free rate per unit of volatility. The Sharpe ratio is calculated as $(R_p - R_f)/\sigma_p$, where R_p is the return of portfolio, σ_p is the standard deviation of the portfolio’s excess return, and R_f is the return of a risk-free asset (e.g., a government bond). For a zero-investment portfolio, we can always omit R_f since it requires no equity (Mitra 2009).

In this paper, we adopt the Sharpe ratio as the objective for our portfolio construction problem. Since we cannot always obtain an estimate of the total risk beforehand, we often consider sequential maximization of the Sharpe ratio of the next period. Once we predict the mean vector and the covariance matrix of the population of future returns, the optimal portfolio \mathbf{b}^* can be solved as $\mathbf{b}^* = \lambda^{-1} \Sigma^{-1} \boldsymbol{\mu}$, where λ is a predefined parameter representing the relative risk aversion, Σ is the estimated covariance matrix, and $\boldsymbol{\mu}$ is the estimated mean vector (Kan and Zhou 2007).¹ Therefore, predicting the mean and the covariance is essential to construct risk averse portfolios.

3 Proposed System

In this section, we present the details of our proposed system, which is outlined in Figure 1. Our system consists of three parts. In the first part (i), the system extracts residual

¹Note that \mathbf{b}^* is derived as the maximizer of $\mathbf{b}^\top \boldsymbol{\mu} - \frac{\lambda}{2} \mathbf{b}^\top \Sigma \mathbf{b}$, where $\mathbf{b}^\top \boldsymbol{\mu}$ and $\mathbf{b}^\top \Sigma \mathbf{b}$ are the return and the risk of the portfolio \mathbf{b} , respectively.

information to hedge out the effects of common market factors. To this end, in Section 3.1, we introduce the *spectral residual*, a novel method based on spectral decomposition. In the second part (ii), the system predicts future distributions of the spectral residuals using a neural network-based predictor. In the third part (iii), the predicted distributional information is leveraged for constructing optimal portfolios. We will outline these procedures in Section 3.2. Additionally, we introduce a novel network architecture that incorporates well-known financial inductive biases, which we explain in Section 3.3.

3.1 Extracting residual factors

As mentioned in the introduction, we focus on developing trading strategy based on the residual factors, i.e., the information remaining after hedging out the common market factors. Here, we introduce a novel method to extract the residual information, which we call the *spectral residual*.

Definition of the spectral residuals First, we introduce some notions from portfolio theory. Let \mathbf{r} be a random vector with zero mean and covariance $\Sigma \in \mathbb{R}^{S \times S}$, which represents the returns of S stocks over the given investment horizon. Since Σ is symmetric, we have a decomposition $\Sigma = \mathbf{V} \Lambda \mathbf{V}^\top$, where $\mathbf{V} = [\mathbf{v}_1, \dots, \mathbf{v}_S]$ is an orthogonal matrix and $\Lambda = \text{diag}(\lambda_1, \dots, \lambda_S)$ is a diagonal matrix of the eigenvalues. Then, we can create a new random vector as $\hat{\mathbf{r}} = \mathbf{V}^\top \mathbf{r}$ such that the coordinate variables $\hat{r}_i = \mathbf{v}_i^\top \mathbf{r}$ are mutually uncorrelated. In portfolio theory, \hat{r}_i s are called *principal portfolios* (Partovi and Caputo 2004). Principal portfolios have been utilized in “risk parity” approaches to diversify the exposures to the intrinsic source of risk in the market (Meucci 2009).

Since the volatility (i.e., the standard deviation) of the i -th principal portfolio is given as $\sqrt{\lambda_i}$, the raw return sequence has large exposure to the principal portfolios with large eigenvalues. For example, the first principal portfolio can be seen as the factor that corresponds to the overall market (Meucci 2009). Therefore, to hedge out common market factors, a natural idea is to discard several principal portfolios with largest eigenvalues. Formally, we define the spectral residuals as follows.

Definition 2. Let $C (< S)$ be a given positive integer. We define the spectral residual $\tilde{\mathbf{e}}$ as a vector obtained by projecting the raw return vector \mathbf{r} onto the space spanned by the principal portfolios with the smallest $S - C$ eigenvalues.

In practice, we calculate the empirical version of the spectral residuals as follows. Given a time window $H > 1$, we define a windowed signal \mathbf{X}_t as $\mathbf{X}_t := [\mathbf{r}_{t-H}, \dots, \mathbf{r}_{t-1}]$. We also denote by $\tilde{\mathbf{X}}_t$ a matrix obtained by subtracting empirical means of row vectors from \mathbf{X}_t . By the singular value decomposition (SVD), $\tilde{\mathbf{X}}_t$ can be decomposed as

$$\tilde{\mathbf{X}}_t = \mathbf{V}_t \underbrace{\text{diag}(\sigma_1, \dots, \sigma_S)}_{\text{principal portfolios}} \mathbf{U}_t,$$

where \mathbf{V}_t is an $S \times S$ orthogonal matrix, \mathbf{U}_t is an $S \times H$ matrix whose rows are mutually orthogonal unit vectors, and $\sigma_1 \geq \dots \geq \sigma_S$ are singular values. Note that $\mathbf{V}_t^\top \tilde{\mathbf{X}}_t$ can be seen as the realized returns of the principal portfolios. Then, the (empirical) spectral residual at time s ($t-H \leq s \leq t-1$) is computed as

$$\tilde{\epsilon}_s := \mathbf{A}_t \mathbf{r}_s, \quad (2)$$

where \mathbf{A}_t is the projection matrix defined as

$$\mathbf{A}_t := \mathbf{V}_t \text{diag}(\underbrace{0, \dots, 0}_C, \underbrace{1, \dots, 1}_{S-C}) \mathbf{V}_t^\top.$$

Relationship to factor models Although we defined the spectral residuals through PCA, they are also related to the generative model (1), and thus convey information about “residual factors” in the original sense.

In the finance literature, it has been pointed out that trading strategies depending only on the residual factor ϵ_t in (1) can be robust to structural changes in the overall market (Blitz, Huij, and Martens 2011; Blitz et al. 2013). While estimating parameters in the linear factor model (1) is typically done by factor analysis (FA) methods (Bartholomew, Knott, and Moustaki 2011), the spectral residual $\tilde{\epsilon}_t$ is not exactly the same as the residual factors obtained from the FA. Despite this, we can show the following result that the spectral residuals can hedge out the common market factors under a suitable condition.

Proposition 1. Let \mathbf{r} be a random vector in \mathbb{R}^S generated according to a linear model $\mathbf{r} = \mathbf{B}\mathbf{f} + \epsilon$, where \mathbf{B} is an $S \times C$ matrix, and $\mathbf{f} \in \mathbb{R}^C$ and $\epsilon \in \mathbb{R}^S$ are zero-mean random vectors. Assume that the following conditions hold:

- $\text{Var}(f_i) = 1$ and $\text{Var}(\epsilon_k) = \sigma > 0$.
- The coordinate variables in \mathbf{f} and ϵ are uncorrelated, that is, $\mathbb{E}[f_i f_j] = 0$, $\mathbb{E}[\epsilon_k \epsilon_\ell] = 0$, and $\mathbb{E}[f_i \epsilon_k] = 0$ hold for any $i \neq j$ and $k \neq \ell$.

Then, we have the followings.

- (i) The spectral residual $\tilde{\epsilon}$ defined in (2) is uncorrelated from the common factor \mathbf{f} .
- (ii) The covariance matrix of $\tilde{\epsilon}$ is given as $\sigma^2 \mathbf{A}_{\text{res}}$. Under a suitable assumption², this can be approximated as a diagonal matrix, which means the coordinates variables of the spectral residual ϵ_i ($i \in \{1, \dots, S\}$) are almost uncorrelated.

²See Appendix B for a precise statement.

In the above proposition, the first statement (i) claims that the spectral residual can eliminate the common factors without knowing the exact residual factors. The latter statement (ii) justifies the diagonal approximation of the predicted covariance, which will be utilized in the next subsection. For completeness, we provide the proof in Appendix B. Moreover, the assumption that ϵ is isotropic can be relaxed in the following sense. If we assume that the residual factor ϵ is “almost isotropic” and the common factors $\mathbf{B}\mathbf{f}$ have larger volatility contributions than ϵ , we can show that the linear transformation used in the spectral residual is close to the projection matrix eliminating the market factors. Since the formal statement is somewhat involved, we give the details in Appendix B.

Besides, the spectral residual can be computed significantly faster than the FA-based methods. This is because the FA typically requires iterative executions of the SVD to solve a non-convex optimization problem, while the spectral residual requires it only once. Section 4.2 gives an experimental comparison of running times.

3.2 Distributional prediction and portfolio construction

Our next goal is to construct a portfolio based on the extracted information. To this end, we here introduce a method to forecast future distributions of the spectral residuals, and explain how we can convert the distributional features into executable portfolios.

Distributional prediction Given a sequence of past realizations of residual factors, $\tilde{\epsilon}_{i,t-H}, \dots, \tilde{\epsilon}_{i,t-1}$, consider the problem of predicting the distribution of a future observation $\tilde{\epsilon}_{i,t}$. Our approach is to learn a functional predictor for the conditional distribution $p(\tilde{\epsilon}_{i,t} \mid \tilde{\epsilon}_{i,t-H}, \dots, \tilde{\epsilon}_{i,t-1})$. Since our final goal is to construct the portfolio, we only use predicted means and covariances, and we do not need the full information about the conditional distribution. Despite this, fitting symmetric models such as Gaussian distributions can be problematic because it is known that the distributions of returns are often skewed (Cont 2000; Lin and Liu 2018). To circumvent this, we utilize quantile regression (Koenker 2005), an off-the-shelf nonparametric method to estimate conditional quantiles. Intuitively, if we obtain a sufficiently large number of quantiles of the target variable, we can reconstruct any distributional properties of that variable. We train a function ψ that predicts several conditional quantile values, and convert its output into estimators of conditional means and variances. The overall procedure can be made to be differentiable, so we can incorporate it into modern deep learning frameworks.

Here, we provide the details of the aforementioned procedure. First, we give an overview for the quantile regression objective. Let Y be a scalar-valued random variable, and \mathbf{X} be another random variable. For $\alpha \in (0, 1)$, an α -th conditional quantile of Y given $\mathbf{X} = \mathbf{x}$ is defined as

$$y(\mathbf{x}; \alpha) := \inf\{y' : P(Y \leq y' \mid \mathbf{X} = \mathbf{x}) \geq \alpha\}.$$

It is known that $y(\mathbf{x}; \alpha)$ can be found by solving the follow-

ing minimization problem

$$y(\mathbf{x}; \alpha) = \operatorname{argmin}_{y' \in \mathbb{R}} \mathbb{E}[\ell_\alpha(Y, y') \mid \mathbf{X} = \mathbf{x}],$$

where $\ell_\alpha(y, y')$ is the pinball loss defined as

$$\ell_\alpha(y, y') := \max\{(\alpha - 1)(y - y'), \alpha(y - y')\}.$$

For our situation, the target variable is $y_t = \tilde{\epsilon}_{i,t}$ and the explanatory variable is $\mathbf{x}_t = (\tilde{\epsilon}_{i,t-H}, \dots, \tilde{\epsilon}_{i,t-1})^\top$. We want to construct a function $\psi : \mathbb{R}^H \rightarrow \mathbb{R}$ that estimate the conditional α -quantile of y_t . To this end, the quantile regression tries to solve the following minimization problem

$$\min_{\psi} \widehat{\mathbb{E}}_{y_t, \mathbf{x}_t}[\ell_\alpha(y_t, \psi(\mathbf{x}_t))].$$

Here, $\widehat{\mathbb{E}}_{y_t, \mathbf{x}_t}$ is understood as taking the empirical expectation with respect to y_t and \mathbf{x}_t across t . We should note that a similar application of the quantile regression to forecasting conditional quantiles of time series has been considered in (Biau and Patra 2011).

Next, let $Q > 0$ be a given integer, and let $\alpha_j = j/Q$ ($j = 1, \dots, Q - 1$) be an equispaced grid of quantiles. We consider the problem of simultaneously estimating α_j -quantiles by a function $\psi : \mathbb{R}^H \rightarrow \mathbb{R}^{Q-1}$. To do this, we define a loss function as

$$\mathcal{L}_Q(y_t, \psi(\mathbf{x}_t)) := \sum_{j=1}^{Q-1} \ell_{\alpha_j}(y_t, \psi_j(\mathbf{x}_t)),$$

where $\psi_j(\mathbf{x}_t)$ is the j -th coordinate of $\psi(\mathbf{x}_t)$.

Once we obtain the estimated $Q - 1$ quantiles $\tilde{y}_t^{(j)} = \psi_j(\mathbf{x}_t)$ ($j = 1, \dots, Q - 1$), we can estimate the future mean of the target variable y_t as

$$\hat{\mu}_t := \hat{\mu}(\tilde{\mathbf{y}}_t) = \frac{1}{Q-1} \sum_{j=1}^{Q-1} \tilde{y}_t^{(j)}. \quad (3)$$

Similarly, we can estimate the future variance by the sample variance of $\tilde{y}_t^{(j)}$

$$\hat{\sigma}_t := \hat{\sigma}(\tilde{\mathbf{y}}_t) = \frac{1}{Q-1} \sum (\tilde{y}_t^{(j)} - \hat{\mu}_t)^2 \quad (4)$$

or its robust counterpart such as the median absolute deviation (MAD).

Portfolio construction Given the estimated means and variances of future spectral residuals, we finally construct a portfolio based on optimality criteria offered by modern portfolio theory (Markowitz 1952). As mentioned in Section 2.2, the formula for the optimal portfolio requires the means and the covariances of the returns. Thanks to Proposition 1-(ii), we can approximate the covariance matrix of the spectral residual by a diagonal matrix. Precisely, once we calculate the predicted mean $\hat{\mu}_{t,j}$ and the variance $\hat{\sigma}_{t,j}^2$ of the spectral residual at time t , the weight for j -th asset is given as $b_j := \lambda^{-1} \hat{\mu}_{t,j} / \hat{\sigma}_{t,j}^2$.

In the experiments in Section 4, we compare the performances of zero-investment portfolios. For trading strategies

that do not output zero-investment portfolios, we apply a common transformation to portfolios to be centered and normalized. As a result, the eventual portfolio does not depend on the risk aversion parameter λ . See Appendix A.1 for details.

3.3 Network architectures

For the model of the quantile predictor ψ , we introduce two architectures for neural network models that take into account scale invariances studied in finance.

Volatility invariance First, we consider an invariance property on amplitudes of financial time series. It is known that financial time series data exhibit a property called volatility clustering (Mandelbrot 1997). Roughly speaking, volatility clustering describes a phenomenon that large changes in financial time series tend to be followed by large changes, while small changes tend to be followed by small changes. As a result, if we could observe a certain signal as a financial time series, a signal obtained by positive scalar multiplication can be regarded as another plausible realization of a financial time series.

To incorporate such an amplitude invariance property into the model architectures, we leverage the class of positive homogeneous functions. Here, a function $f : \mathbb{R}^n \rightarrow \mathbb{R}^m$ is said to be positive homogeneous if $f(a\mathbf{x}) = af(\mathbf{x})$ holds for any $\mathbf{x} \in \mathbb{R}^n$ and $a > 0$. For example, we can see that any linear functions and any ReLU neural networks with no bias terms are positive homogeneous. More generally, we can model the class of positive homogeneous functions as follows. Let $\tilde{\psi} : S^{H-1} \rightarrow \mathbb{R}^{Q-1}$ be any function defined on the $H - 1$ dimensional sphere $S^{H-1} = \{\mathbf{x} \in \mathbb{R}^H : \|\mathbf{x}\| = 1\}$. Then, we obtain a positive homogeneous function as

$$\psi(\mathbf{x}) = \|\mathbf{x}\| \tilde{\psi} \left(\frac{\mathbf{x}}{\|\mathbf{x}\|} \right). \quad (5)$$

Thus, we can convert any function class on the sphere into the model of amplitude invariant predictors.

Time-scale invariance Second, we consider an invariance property with respect to time-scale. There is a well-known hypothesis that time series of stock prices have *fractal structures* (Peters 1994). The fractal structure refers to a self-similarity property of a sequence. That is, if we observe a single sequence in several different sampling rates, we cannot infer the underlying sampling rates from the shape of downsampled sequences. The fractal structure has been observed in several real markets (Cao, Cao, and Xu 2013; Mensi et al. 2018; Lee et al. 2018). See Remark 1 in Appendix A.2 for further discussion on this property.

To take advantage of the fractal structure, we propose a novel network architecture that we call *fractal networks*. The key idea is that we can effectively exploit the self-similarity by applying a single common operation to multiple subsequences with different resolutions. By doing so, we expect that we can increase sample efficiency and reduce the number of parameters to train.

Here, we give a brief overview of the proposed architecture, while a more detailed explanation will be given in Ap-

pendix A.2. Our model consists of (a) the resampling mechanism and (b) two neural networks ψ_1 and ψ_2 . The input-output relation of our model is described as the following procedure. First, given a single sequence \mathbf{x} of stock returns, the resampling mechanism $\text{Resample}(\mathbf{x}, \tau)$ generates a sequence that corresponds to sampling rates specified by a scale parameter $0 < \tau \leq 1$. We apply Resample procedure for L different parameters $\tau_1 < \dots < \tau_L = 1$ and generate L sequences. Next, we apply a common non-linear transformation ψ_1 modeled by a neural network. Finally, by taking the empirical mean of these sequences, we aggregate the information on different sampling rates and apply another network ψ_2 . To sum up, the overall procedure can be written in the following single equation

$$\psi(\mathbf{x}) = \psi_2 \left(\frac{1}{L} \sum_{i=1}^L \psi_1(\text{Resample}(\mathbf{x}, \tau_i)) \right). \quad (6)$$

4 Experiments

We conducted a series of experiments to demonstrate the effectiveness of our methods on real market data. In Section 4.1, we describe the details of the dataset and some common experimental settings used throughout this section. In Section 4.2, we test the validity of the spectral residual by a preliminary experiment. In Section 4.3, we evaluate the performance of our proposed system by experiments on U.S. market data. We also conducted similar experiments on Japanese market data and obtained consistent results. Due to the space limitation, we provide the entire results for Japanese market data in Appendix E.

4.1 Dataset description and common settings

U.S. market data For U.S. market data, we used the daily prices of stocks listed in S&P 500 from January 2000 to April 2020. We used data before January 2008 for training and validation and the remainder for testing. We obtained the data from Alpha Vantage³.

We used opening prices because of the following reasons. First, the trading volume at the opening session is larger than that at the closing session (Amihud and Mendelson 1987), which means that trading with opening prices is practically easier than trading with the closing prices. Moreover, a financial institution cannot trade a large amount of stocks during the closing period because it can be considered as an illegal action known as “banging the close”.

Common experimental settings We adopted the delay parameter $d = 1$ (i.e., one-day delay) for updating portfolios. We set the look-back window size as $H = 256$, i.e., all prediction models can access the historical stock prices up to preceding 256 business days. For other parameters used in the experiments, see Appendix C.3 as well.

Evaluation metrics We list the evaluation metrics used throughout our experiments.

- *Cumulative Wealth (CW)* is the total return yielded from the trading strategy: $CW_T := \prod_{i=1}^T (1 + R_t)$.

³<https://www.alphavantage.co/>

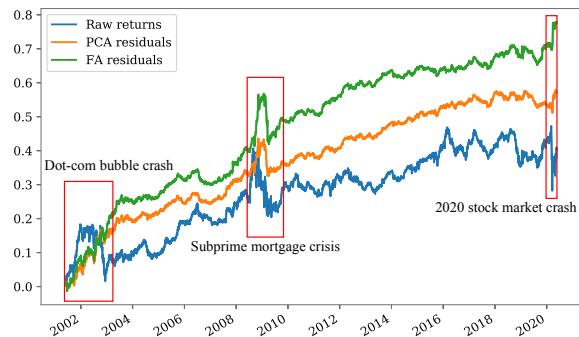


Figure 2: Cumulative returns of reversal strategies over raw returns, the FA residuals, and the spectral residuals. The reversal-based strategies are more robust against financial crises.

- *Annualized Return (AR)* is an annualized return rate defined as $AR_t := (T_Y/T) \sum_{i=1}^T R_t$, where T_Y is the average number of holding periods in a year.
- *Annualized Volatility (AVOL)* is annualized risk defined as $AVOL_T := ((T_Y/T) \sum_{i=1}^T R_t^2)^{1/2}$.
- *Annualized Sharpe ratio (ASR)* is an annualized risk-adjusted return (Sharpe 1994). It is defined as $ASR_T := AR_T / AVOL_T$.

As mentioned in Section 2.2, we are mainly interested in ASR as the primary evaluation metric. AR and AVOL are auxiliary metrics for calculating ASR. While CW represents the actual profits, it often ignores the existence of large risk values. In addition to these, we also calculated some evaluation criteria commonly used in finance: Maximum Draw-Down (MDD), Calmar Ratio (CR), and Downside Deviation Ratio (DDR). For completeness, we provide precise definitions in Appendix C.1.

4.2 Validity of spectral residuals

As suggested in 3.1, the spectral residuals can be useful to hedge out the undesirable exposure to the market factors. To verify this, we compared the performances of trading strategies over (i) the raw returns, (ii) the residual factors extracted by the factor analysis (FA), and (iii) the spectral residuals.

For the FA, we fit the factor model (1) with $K = 30$ by the maximum likelihood method (Bartholomew, Knott, and Moustaki 2011) and extracted residual factors as the remaining part. For the spectral residual, we obtain the residual sequence by subtracting $C = 30$ principal components from the raw returns. We applied both methods to windowed data with length $H = 256$.

In order to be agnostic to the choice of training algorithms, we used a simple reversal strategy. Precisely, for the raw return sequence r_t , we used a deterministic strategy obtained simply by normalizing the negation of the previous observation $-r_{t-1}$ to be a zero-investment portfolio (see Appendix C.2 for the precise formula). We defined reversal strategies over residual sequences in similar ways.

Figure 2 shows the cumulative returns of reversal strategies performed on the Japanese market data. We see that the

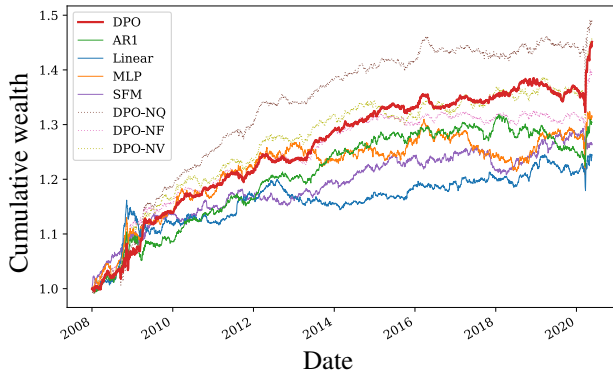


Figure 3: The Cumulative Wealth in U.S. market.

reversal strategy based on the raw returns is significantly affected by several well-known financial crises, including the dot-com bubble crash in the early 2000s, the 2008 subprime mortgage crisis, and the 2020 stock market crash. On the other hand, two residual-based strategies seem to be more robust against these financial crises. The spectral residual performed similarly to the FA residual in cumulative returns. Moreover, in terms of the Sharpe ratio, the spectral residuals ($= 2.86$) performed better than the FA residuals ($= 2.64$).

Remarkably, the spectral residuals were calculated much faster than the FA residuals. In particular, we calculated both residuals using the entire dataset which contains records of all the stock prices for 5,000 days. For the PCA and the FA, we used implementations in the scikit-learn package (Pedregosa et al. 2011), and all the computation were run on 18 CPU cores of Intel Xeon Gold 6254 Processor (3.1 GHz). Then, extracting the spectral residuals took approximately 10 minutes, while the FA took approximately 13 hours.

4.3 Performance evaluation of the proposed system

We evaluated the performance of our proposed system described in Section 3 on U.S. market data. Corresponding results for Japanese market data are provided in Appendix E.

Baseline Methods We compare our system with the following baselines: (i) `Market` is the uniform buy-and-hold strategy. (ii) `AR(1)` is the AR(1) model with all coefficients being -1 . This can be seen as the simple reversal strategy. (iii) `Linear` predicts returns by ordinary linear regression based on previous H raw returns. (iv) `MLP` predicts returns by a multi-layer perceptron with batch normalization and dropout (Pal and Mitra 1992; Ioffe and Szegedy 2015; Srivastava et al. 2014). (v) `SFM` is one of state-of-the-art stock price prediction algorithms based on the State Frequency Memory RNNs (Zhang, Aggarwal, and Qi 2017).

Additionally, we compare our proposed system (DPO) with some ablation models, which are similar to DPO except for the following points.

- DPO with No Quantile Prediction (DPO-NQ) does not use the information of the full distributional prediction, but in-

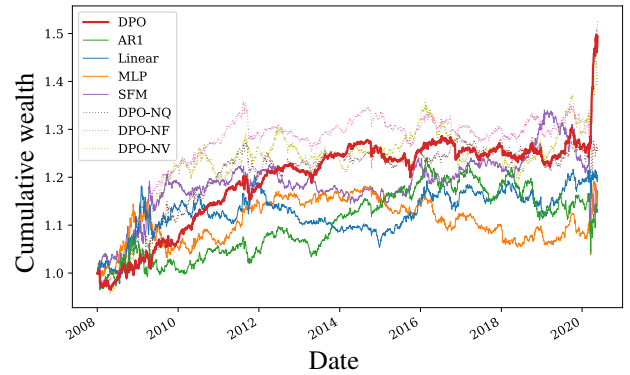


Figure 4: The Cumulative Wealth in U.S. market data without spectral residual extraction.

Table 1: Performance comparison on U.S. market. All the methods except for `Market` are applied to the spectral residuals (SRes).

	ASR \uparrow	AR \uparrow	AVOL \downarrow	DDR \uparrow	CR \uparrow	MDD \downarrow
Market	+0.607	+0.130	0.215	+0.939	+0.263	0.496
AR(1) on SRes	+0.858	+0.021	0.025	+1.470	+0.295	0.072
Linear on SRes	+0.724	+0.017	0.024	+1.262	+0.298	0.059
MLP on SRes	+0.728	+0.022	0.030	+1.280	+0.283	0.077
SFM on SRes	+0.709	+0.019	0.026	+1.211	+0.323	0.058
DPO-NQ	+1.237	+0.032	0.026	+2.169	+0.499	0.063
DPO-NF	+1.284	+0.027	0.021	+2.347	+0.627	0.042
DPO-NV	+1.154	+0.030	0.026	+2.105	+0.562	0.053
DPO (Proposed)	+1.393	+0.030	0.021	+2.561	+0.656	0.045

stead it outputs conditional means trained by the L_2 loss.

- DPO with No Fractal Network (DPO-NF) uses a simple multi-layer perceptron instead of the fractal network.
- DPO with No Volatility Normalization (DPO-NV) does not use the normalization (5) in the fractal network.

Performance on real market data Figure 3 shows the cumulative wealth (CW) achieved in U.S. market. Table 1 shows the results for the other evaluation metrics presented in Section 4.1. For parameter C of the spectral residual, we used $C = 10$, which we determined solely from the training data (see Appendix D.2 for details). Overall, our proposed method DPO outperformed the baseline methods in multiple evaluation metrics. Regarding the comparison against three ablation models, we make the following observations.

1. **Effect of the distributional prediction.** We found that introducing the distributional prediction significantly improved the ASR. While DPO-NQ achieved the best CW, DPO performed better in the ASR. It suggests that, without the variance prediction, DPO-NQ tends to pursue the returns without regard to taking the risks. Generally, we observed that DPO reduced the AVOL while not losing the AR.

Table 2: Performance comparison on U.S. market without spectral residual extraction.

	ASR \uparrow	AR \uparrow	AVOL \downarrow	DDR \uparrow	CR \uparrow	MDD \downarrow
AR(1)	+0.212	+0.011	0.051	+0.355	+0.067	0.160
Linear	+0.304	+0.016	0.052	+0.485	+0.127	0.125
MLP	+0.261	+0.013	0.048	+0.424	+0.103	0.122
SFM	+0.264	+0.014	0.051	+0.428	+0.079	0.171
DPO-NQ	+0.405	+0.020	0.048	+0.655	+0.172	0.114
DPO-NF	+0.854	+0.034	0.040	+1.472	+0.436	0.078
DPO-NV	+0.542	+0.029	0.054	+0.922	+0.238	0.123
DPO	+0.874	+0.032	0.037	+1.485	+0.524	0.061

2. **Effect of the fractal network.** Introducing the fractal network architecture also improved the performance in multiple evaluation metrics. In both markets, we observed that the fractal network contributed to increasing the AR while keeping the AVOL, which is suggestive of the effectiveness of leveraging the financial inductive bias on the return sequence.
3. **Effect of the normalization.** We also saw the effectiveness of the normalization (5). Comparing DPO and DPO-NV, the normalization affected both of the AR and the AVOL, resulting in the improvement in the ASR. This may occur because the normalization improves the sample efficiency by reducing the degrees of freedom of the model.

To see the effect of the spectral residuals, we also evaluated our proposed method and the baseline methods on the raw stock returns. Figure 4 and Table 2 show the results. Compared to the corresponding results with spectral residuals, we found that the spectral residuals consistently improved the performance for every method. Some further intriguing observations are summarized as follows.

1. With the spectral residuals, AR(1) achieved the best ASR among the baseline methods (Table 1), which has not been observed on the raw return sequence (Table 2). This suggests that the spectral residuals encourage the reversal phenomenon (Poterba and Summers 1988) by suppressing the common market factors. Interestingly, without extracting the spectral residuals, the CWs are crossing during the test period, and no single baseline method consistently beats others (Figure 4). A possible reason is that the strong correlation between the raw stock returns increases the exposure to the common market risks.
2. We found that our network architectures are still effective on the raw sequences. In particular, DPO outperformed all the other methods in multiple evaluation metrics.

5 Related Work

5.1 Factor Models and Residual Factors

Trading based on factor models is one of the popular strategies for quantitative portfolio management (e.g., (Nakagawa, Uchida, and Aoshima 2018)). One of the best-known factor models is Fama and French (Fama and French 1992,

1993), and they put forward a model explaining returns in the US equity market with three factors: the market return factor, the size (market capitalization) factor and the value (book-to-market) factor.

Historically, residual factors are treated as errors in factor models (Sharpe 1964). However, (Blitz, Huij, and Martens 2011; Blitz et al. 2013) suggested that there exists predictability in residual factors. In modern portfolio theory, less correlation of investment returns enables to earn larger risk-adjusted returns (Markowitz 1952). Residual factors are less correlated than the raw stock returns by its nature. Consequently, (Blitz, Huij, and Martens 2011; Blitz et al. 2013) demonstrated that residual factors enable to earn larger risk-adjusted returns.

5.2 Asset Price Prediction using Deep Learning

With the recent advance of deep learning, various deep neural networks are applied to stock price prediction (Chen et al. 2019). Some deep neural networks for time series are also applied to stock price prediction (Fischer and Krauss 2018).

Compared to other classical machine learning methods, deep learning enables learning with fewer a priori representational assumptions if provided with sufficient amount of data and computational resources. Even if data is insufficient, introducing inductive biases to a network architecture can still facilitate deep learning (Battaglia et al. 2018). Technical indicators are often used for stock prediction (e.g., (Metghalchi, Marcucci, and Chang 2012; Neely et al. 2014)), and (Li et al. 2019) used technical indicators as inductive biases of a neural network. (Zhang, Aggarwal, and Qi 2017) used a recurrent model that can analyze frequency domains so as to distinguish trading patterns of various frequencies.

6 Conclusions

We proposed a system for constructing portfolios. The key technical ingredients are (i) a spectral decomposition-based method to hedge out common market factors and (ii) a distributional prediction method based on a novel neural network architecture incorporating financial inductive biases. Through empirical evaluations on the real market data, we demonstrated that our proposed method can significantly improve the performance of portfolios on multiple evaluation metrics. Moreover, we verified that each of our proposed techniques is effective on its own, and we believe that our techniques may have wide applications in various financial problems.

Acknowledgment

We thank the anonymous reviewers for their constructive suggestions and comments. We also thank Masaya Abe, Shuhei Noma, Prabhat Nagarajan and Takuya Shimada for helpful discussions.

References

Amihud, Y.; and Mendelson, H. 1987. Trading mechanisms and stock returns: An empirical investigation. *The Journal of Finance* 42(3): 533–553.

- Bartholomew, D.; Knott, M.; and Moustaki, I. 2011. *Latent Variable Models and Factor Analysis: A Unified Approach*. Wiley, 3rd edition.
- Battaglia, P. W.; Hamrick, J. B.; Bapst, V.; Sanchez-Gonzalez, A.; Zambaldi, V.; Malinowski, M.; Tacchetti, A.; Raposo, D.; Santoro, A.; Faulkner, R.; et al. 2018. Relational inductive biases, deep learning, and graph networks. *arXiv preprint arXiv:1806.01261*.
- Biau, G.; and Patra, B. 2011. Sequential Quantile Prediction of Time Series. *IEEE Transactions on Information Theory* 57(3): 1664–1674.
- Blitz, D.; Huij, J.; Lansdorp, S.; and Verbeek, M. 2013. Short-term residual reversal. *Journal of Financial Markets* 16(3): 477–504.
- Blitz, D.; Huij, J.; and Martens, M. 2011. Residual momentum. *Journal of Empirical Finance* 18(3): 506–521.
- Calomiris, C. W.; Love, I.; and Peria, M. S. M. 2010. Crisis’ Shock Factors’ and the Cross-Section of Global Equity Returns. Technical report, National Bureau of Economic Research.
- Cao, G.; Cao, J.; and Xu, L. 2013. Asymmetric multifractal scaling behavior in the Chinese stock market: Based on asymmetric MF-DFA. *Physica A: Statistical Mechanics and its Applications* 392(4): 797–807.
- Chen, C.; Zhao, L.; Bian, J.; Xing, C.; and Liu, T.-Y. 2019. Investment behaviors can tell what inside: Exploring stock intrinsic properties for stock trend prediction. In *Proceedings of the 25th ACM SIGKDD International Conference on Knowledge Discovery & Data Mining*, 2376–2384.
- Choudhry, R.; and Garg, K. 2008. A hybrid machine learning system for stock market forecasting. *World Academy of Science, Engineering and Technology* 39(3): 315–318.
- Cont, R. 2000. Empirical properties of asset returns: stylized facts and statistical issues. *Quantitative Finance* 1: 223–236.
- Davis, C.; and Kahan, W. M. 1970. The Rotation of Eigenvectors by a Perturbation. III. *SIAM Journal on Numerical Analysis* 7(1): 1–46.
- Devlin, J.; Chang, M.-W.; Lee, K.; and Toutanova, K. 2019. BERT: Pre-training of Deep Bidirectional Transformers for Language Understanding. In *NAACL-HLT*.
- Fama, E. F.; and French, K. R. 1992. The Cross-Section of Expected Stock Returns. *The Journal of Finance* 47(2): 427–465.
- Fama, E. F.; and French, K. R. 1993. Common risk factors in the returns on stocks and bonds. *Journal of*.
- Fama, E. F.; and French, K. R. 2015. A five-factor asset pricing model. *Journal of Financial Economics* 116(1): 1–22.
- Fischer, T.; and Krauss, C. 2018. Deep learning with long short-term memory networks for financial market predictions. *European Journal of Operational Research* 270(2): 654–669.
- Graves, A.; Mohamed, A.; and Hinton, G. 2013. Speech recognition with deep recurrent neural networks. In *2013 IEEE International Conference on Acoustics, Speech and Signal Processing*, 6645–6649. ISSN 2379-190X.
- Grossman, S. J.; and Zhou, Z. 1993. Optimal investment strategies for controlling drawdowns. *Mathematical finance* 3(3): 241–276.
- Hochreiter, S.; and Schmidhuber, J. 1997. Long Short-Term Memory. *Neural Computation* 9(8): 1735–1780.
- Ioffe, S.; and Szegedy, C. 2015. Batch normalization: Accelerating deep network training by reducing internal covariate shift. *arXiv preprint arXiv:1502.03167*.
- Jegadeesh, N.; and Titman, S. 1993. Returns to Buying Winners and Selling Losers: Implications for Stock Market Efficiency. *The Journal of Finance* 48(1): 65–91.
- Kan, R.; and Zhou, G. 2007. Optimal portfolio choice with parameter uncertainty. *Journal of Financial and Quantitative Analysis* 42(3): 621–656.
- Kingma, D. P.; and Ba, J. 2015. Adam: A Method for Stochastic Optimization. In *International Conference for Learning Representations (ICLR)*.
- Kintzel, D. 2007. Portfolio theory, life-cycle investing, and retirement income. *Social Security Administration Policy Brief* 2007-02.
- Koenker, R. 2005. *Quantile Regression*. Econometric Society Monographs. Cambridge University Press. doi:10.1017/CBO9780511754098.
- Krauss, C.; Do, X. A.; and Huck, N. 2017. Deep neural networks, gradient-boosted trees, random forests: Statistical arbitrage on the S&P 500. *European Journal of Operational Research* 259(2): 689–702.
- Kristoufek, L.; and Vosvrda, M. 2014. Measuring capital market efficiency: long-term memory, fractal dimension and approximate entropy. *The European Physical Journal B* 87(7): 162.
- Krizhevsky, A.; Sutskever, I.; and Hinton, G. E. 2012. ImageNet Classification with Deep Convolutional Neural Networks. In Pereira, F.; Burges, C. J. C.; Bottou, L.; and Weinberger, K. Q., eds., *Advances in Neural Information Processing Systems* 25, 1097–1105. Curran Associates, Inc. URL <http://papers.nips.cc/paper/4824-imagenet-classification-with-deep-convolutional-neural-networks.pdf>.
- LeCun, Y.; Haffner, P.; Bottou, L.; and Bengio, Y. 1999. Object Recognition with Gradient-Based Learning. In *Shape, Contour and Grouping in Computer Vision*, 319–345. Springer Berlin Heidelberg.
- Lee, M.; Song, J.; Kim, S.; and Chang, W. 2018. Asymmetric market efficiency using the index-based asymmetric-MFDFA. *Physica A: Statistical Mechanics and its Applications* 512(15): 1278–1294.
- Li, Z.; Yang, D.; Zhao, L.; Bian, J.; Qin, T.; and Liu, T.-Y. 2019. Individualized indicator for all: Stock-wise technical indicator optimization with stock embedding. In *Proceedings of the 25th ACM SIGKDD International Conference on Knowledge Discovery & Data Mining*, 894–902.

- Lin, T.-C.; and Liu, X. 2018. Skewness, individual investor preference, and the cross-section of stock returns. *Review of Finance* 22(5): 1841–1876.
- Lux, T.; and Marchesi, M. 2000. Volatility clustering in financial markets: a microsimulation of interacting agents. *International journal of theoretical and applied finance* 3(04): 675–702.
- Malkiel, B. G.; and Fama, E. F. 1970. Efficient capital markets: A review of theory and empirical work. *The journal of Finance* 25(2): 383–417.
- Mandelbrot, B. B. 1997. The variation of certain speculative prices. In *Fractals and scaling in finance*, 371–418. Springer.
- Mandelbrot, B. B.; and Ness, J. W. V. 1968. Fractional Brownian Motions, Fractional Noises and Applications. *SIAM Review* 10(4): 422–437.
- Markowitz, H. 1952. Portfolio selection. *The journal of finance* 7(1): 77–91.
- Mensi, W.; Hamdi, A.; Shahzad, S. J. H.; Shafiullah, M.; and Al-Yahyaee, K. H. 2018. Modeling cross-correlations and efficiency of Islamic and conventional banks from Saudi Arabia: Evidence from MF-DFA and MF-DXA approaches. *Physica A: Statistical Mechanics and its Applications* 502(15): 576–589.
- Metghalchi, M.; Marcucci, J.; and Chang, Y.-H. 2012. Are moving average trading rules profitable? Evidence from the European stock markets. *Applied Economics* 44(12): 1539–1559.
- Meucci, A. 2009. Managing Diversification. *Risk* 22(5): 74–79.
- Mitra, S. K. 2009. Optimal combination of trading rules using neural networks. *International business research* 2(1): 86–99.
- Nakagawa, K.; Uchida, T.; and Aoshima, T. 2018. Deep factor model. In *ECML PKDD 2018 Workshops*, 37–50. Springer.
- Neely, C. J.; Rapach, D. E.; Tu, J.; and Zhou, G. 2014. Forecasting the equity risk premium: the role of technical indicators. *Management science* 60(7): 1772–1791.
- Pal, S. K.; and Mitra, S. 1992. Multilayer perceptron, fuzzy sets, classification. *IEEE Transactions on Neural Networks* 3(5): 683–697.
- Partovi, M. H.; and Caputo, M. 2004. Principal portfolios: recasting the efficient frontier. *Economics Bulletin* 7(3): 1–10.
- Pasini, G. 2017. Principal component analysis for stock portfolio management. *International Journal of Pure and Applied Mathematics* 115(1): 153–167.
- Pedregosa, F.; Varoquaux, G.; Gramfort, A.; Michel, V.; Thirion, B.; Grisel, O.; Blondel, M.; Prettenhofer, P.; Weiss, R.; Dubourg, V.; Vanderplas, J.; Passos, A.; Cournapeau, D.; Brucher, M.; Perrot, M.; and Duchesnay, E. 2011. Scikit-learn: Machine Learning in Python. *Journal of Machine Learning Research* 12: 2825–2830.
- Peters, E. E. 1994. *Fractal market analysis: applying chaos theory to investment and economics*, volume 24. John Wiley & Sons.
- Poterba, J. M.; and Summers, L. H. 1988. Mean reversion in stock prices: Evidence and Implications. *Journal of Financial Economics* 22(1): 27–59.
- Shah, V. H. 2007. Machine learning techniques for stock prediction. *Foundations of Machine Learning—Spring* 1(1): 6–12.
- Sharpe, W. F. 1964. Capital asset prices: A theory of market equilibrium under conditions of risk. *The journal of finance* 19(3): 425–442.
- Sharpe, W. F. 1994. The sharpe ratio. *Journal of portfolio management* 21(1): 49–58.
- Sortino, F. A.; and Price, L. N. 1994. Performance measurement in a downside risk framework. *the Journal of Investing* 3(3): 59–64.
- Srivastava, N.; Hinton, G.; Krizhevsky, A.; Sutskever, I.; and Salakhutdinov, R. 2014. Dropout: A Simple Way to Prevent Neural Networks from Overfitting. *Journal of Machine Learning Research* 15(56): 1929–1958.
- Szabo, E. 2009. VIX futures and options: A case study of portfolio diversification during the 2008 financial crisis. *The Journal of Alternative Investments* 12(2): 68–85.
- Wang, J.; Zhang, Y.; Tang, K.; Wu, J.; and Xiong, Z. 2019. AlphaStock: A Buying-Winners-and-Selling-Losers Investment Strategy using Interpretable Deep Reinforcement Attention Networks. In *Proceedings of the 25th ACM SIGKDD International Conference on Knowledge Discovery & Data Mining, 1900–1908*.
- Young, T. W. 1991. Calmar ratio: A smoother tool. *Futures* 20(1): 40.
- Yu, Y.; Wang, T.; and Samworth, R. J. 2014. A useful variant of the Davis–Kahan theorem for statisticians. *Biometrika* 102(2): 315–323.
- Zhang, L.; Aggarwal, C.; and Qi, G.-J. 2017. Stock price prediction via discovering multi-frequency trading patterns. In *Proceedings of the 23rd ACM SIGKDD international conference on knowledge discovery and data mining*, 2141–2149.

Appendix

This is the supplementary material for the paper entitled “Deep Portfolio Optimization via Distributional Prediction of Residual Factors”.

A Technical details of the proposed method

In this section, we provide some technical details for our proposed method in Section 3.

A.1 Detailed calculation of portfolio

Let $\boldsymbol{\mu}_t$ be the expected return vector at time t , and $\boldsymbol{\Sigma}_t$ be the covariance matrix of returns. As we explained in Section 2.2, the (ideal) optimal portfolio can be written as $\mathbf{b}_t^* = \lambda^{-1} \boldsymbol{\Sigma}_t^{-1} \boldsymbol{\mu}_t$, where $\lambda > 0$ is a predefined risk aversion parameter. Therefore, having estimators $\hat{\boldsymbol{\mu}}_t$ and $\hat{\boldsymbol{\Sigma}}_t$ for these population quantities, a natural construction of the portfolio is the following plug-in rule

$$\hat{\mathbf{b}}_t := \frac{1}{\lambda} \hat{\boldsymbol{\Sigma}}_t^{-1} \hat{\boldsymbol{\mu}}_t.$$

In our proposed method, we construct a portfolio over the spectral residual $\tilde{\epsilon}_t$. For the estimators of the mean and the covariance, we use the quantile regression-based estimators explained in the previous subsection. In particular, we approximate the covariance matrix by a diagonal matrix $\text{diag}(\hat{\sigma}_{t,1}, \dots, \hat{\sigma}_{t,S})$. See also Appendix B.2 for empirical and theoretical justifications of this diagonal approximation. As a result, the weight for j -th residual factor is given as

$$b_{t,j}^{\text{res}} := \frac{\hat{\mu}_{t,j}}{\lambda \hat{\sigma}_{t,j}},$$

where $\hat{\mu}_{t,j}$ and $\hat{\sigma}_{t,j}$ are predicted means and variances given as (3) and (4), respectively.

We now have a portfolio $\mathbf{b}_t^{\text{res}}$ defined for the spectral residuals. Recall that the spectral residual is obtained as a linear transformation of the (centered) raw returns as $\tilde{\epsilon}_t = \mathbf{A}_t \mathbf{r}_t$ (see Section 3.1). To obtain a portfolio for the raw return \mathbf{r}_t , we use the relation $\mathbf{b}_t = \mathbf{A}_t^\top \mathbf{b}_t^{\text{res}}$.

In our experiment, we apply a common transformation to the output of any trading strategy so that it becomes a zero-investment portfolio. Here, we explain the detail of this transformation. Let \mathbf{b}_t be a given portfolio. Assume that \mathbf{b}_t is not proportional to the all-one vector $\mathbf{1} = (1, \dots, 1)^\top$. This also implies that \mathbf{b}_t is not proportional to the uniform buy-and-hold strategy. To convert \mathbf{b}_t to a zero-investment portfolio, we subtract the average $\bar{b}_t = \frac{1}{S} \sum_{i=1}^S b_{t,i}$ from every coordinate, and then renormalize the portfolio so that the sum of the absolute values is unity. The resulting portfolio is given as

$$\frac{\mathbf{b}_t - \bar{b}_t \mathbf{1}}{\|\mathbf{b}_t - \bar{b}_t \mathbf{1}\|_1}.$$

Note that the normalized portfolio defined in this way does not depend on the parameter λ .

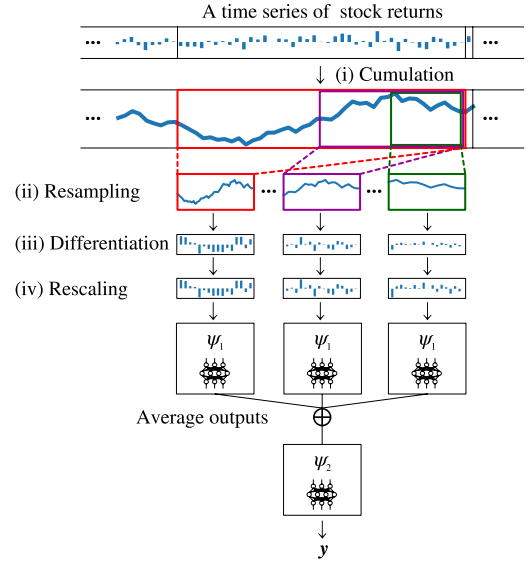


Figure 5: Illustration of the fractal network.

A.2 Fractal networks

Here, we explain the detailed structure of the fractal network introduced in Section 3.3. Figure 5 illustrates the structure of the fractal network.

Let \mathbf{x} denote the input of the network. First, the fractal network applies the resampling mechanism $\text{Resample}(\mathbf{x}, \tau_i)$ for several scale parameters $1 = \tau_0 > \tau_1 > \dots > \tau_L > 0$ to generate multiple views of \mathbf{x} with different sampling rates. To be precise, the resample mechanism outputs a sequence by the following four procedures:

- (i) **Cumulation.** First, given an input $\mathbf{x} = (x_1, \dots, x_H)$, we calculate the cumulative sum $\mathbf{z} = (x_1, x_1 + x_2, \dots, x_1 + \dots + x_H)$. Since the input \mathbf{x} corresponds to the residual factors of the returns, each coordinate variable x_s is understood as the increment or the difference of stock prices of two adjacent time periods. Hence, we use its cumulative sum so that it corresponds to (logarithmic) stock prices and exhibits the fractal structure.
- (ii) **Resampling.** Second, given $0 < \tau \leq 1$ and \mathbf{z} , we generate a shorter sequence \mathbf{z}_τ of a fixed length $H' (< H)$ by downsampling from $(z_{\lfloor (1-\tau)H \rfloor}, \dots, z_H)$. In other words, the resulting sequence is a subsequence with length $\lceil \tau H \rceil$ located at the end of the original sequence.
- (iii) **Differentiation.** Third, we again take the first difference of the downsampled sequence \mathbf{z}_τ to obtain the corresponding return sequence.
- (iv) **Rescaling.** Finally, we normalize the output by multiplying the entire sequence by $\tau^{-1/2}$. On the choice of the multiplicative factor, see following Remark 1 as well.

Next, we apply a common non-linear transformation ψ_1 to these views. Finally, we take average of the results and apply another transformation ψ_2 . The overall procedure is

summarized in the following equation

$$\psi(\mathbf{x}) = \psi_2 \left(\frac{1}{L} \sum_{i=1}^L \psi_1(\text{Resample}(\mathbf{x}, \tau_i)) \right). \quad (7)$$

To incorporate the volatility invariance (Section 3.3) into the fractal network, we want to make the overall transformation $\mathbf{x} \mapsto \psi(\mathbf{x})$ positive homogeneous. To do this, it suffices to ensure that non-linear transformations ψ_1 and ψ_2 are positive homogeneous. This can be proved by combining the following claims.

Lemma 1. Let f_1, f_2, \dots, f_L be any positive homogeneous functions.

- (i) Any linear transformation is positive homogeneous.
- (ii) Suppose the composition $f_1 \circ f_2$ can be defined. Then, $f_1 \circ f_2$ is positive homogeneous.
- (iii) The concatenation $\mathbf{x} \mapsto (f_1(\mathbf{x})^\top, \dots, f_L(\mathbf{x})^\top)^\top$ is positive homogeneous.
- (iv) The average $\mathbf{x} \mapsto \frac{1}{L} \sum_{i=1}^L f_i(\mathbf{x})$ is positive homogeneous.
- (v) The resampling mechanism $\mathbf{x} \mapsto \text{Resample}(\mathbf{x}, \tau)$ is positive homogeneous for any $0 < \tau \leq 1$.

Proof. Since (i), (ii), and (iii) are almost obvious, we omit their proofs. (iv) is derived from (i), (ii), and (iii). As for (v), the resampling mechanism is a linear transformation, and thus it is positive homogeneous. In fact, it is easy to see that the four operations in the resampling mechanism (i.e., cumulation, resampling, differentiation, and rescaling) are linear. Therefore, the resampling mechanism is also linear. \square

Remark 1. In the rescaling phase, the choice of multiplicative factor $\tau^{-1/2}$ is sensible because of the following reason. If the underlying law is the fractional Brownian motion with the Hurst index \mathcal{H} , the appropriate scaling factor determined by its self-similarity is $\tau^{-\mathcal{H}}$ (Mandelbrot and Ness 1968). It has been reported in (Kristoufek and Vosvrda 2014) that, in many real-world markets, estimated Hurst indices are approximately $\mathcal{H} \approx 0.5$, which implies that stock prices exhibit similar self-similarity properties as the standard Brownian motion.

Remark 2. In some paper, the term ‘‘fractal property’’ stands for the behavior of stochastic processes captured by the fractional Brownian motion with $\mathcal{H} \neq 1/2$, which can lead in efficiency of the market. In this paper, however, we focus on the self-similarity of processes to design the network architecture. The self-similarity can be observed even in efficient markets with $\mathcal{H} \approx 0.5$.

B Theoretical analysis

In this section, we provide theoretical analyses of the spectral residuals justifying that the spectral residuals can hedge out the market factors. In Section B.1, we prove Proposition 1, which shows that the spectral residuals are actually uncorrelated to the market factors when the true residual factors are isotropic. In practice, the covariance of the residual factors can be approximated by diagonal matrices. In Section

B.2, we explain why this approximation is justified. In Section B.3, we investigate a more general situation where the true residual factors are anisotropic, i.e., the variances of the coordinate variables differ.

Before proceeding, let us recall the definition of the spectral residual. Let \mathbf{r} be a zero-mean random vector with a covariance matrix $\Sigma \in \mathbb{R}^{S \times S}$. Let $\Sigma = \mathbf{V}\mathbf{\Lambda}\mathbf{V}^\top$ is an eigendecomposition of Σ , where $\mathbf{V} = [\mathbf{v}_1, \dots, \mathbf{v}_S]$ is an orthogonal matrix and $\mathbf{\Lambda} = \text{diag}(\lambda_1, \dots, \lambda_S)$ is a diagonal matrix of the eigenvalues. Assume that $\lambda_1, \dots, \lambda_S$ are sorted in descending order, i.e., $\lambda_1 \geq \dots \geq \lambda_S$. Given an integer $1 \leq C < S$, let

$$\mathbf{V}_{\text{res}} = [\mathbf{v}_{C+1}, \dots, \mathbf{v}_S]$$

be an $S \times (S - C)$ matrix that consists of the eigenvectors that correspond to the smallest $S - C$ eigenvalues⁴. We also define a matrix \mathbf{A}_{res} as

$$\mathbf{A}_{\text{res}} = \mathbf{V}_{\text{res}} \mathbf{V}_{\text{res}}^\top.$$

Note that \mathbf{A}_{res} is the orthogonal projection onto the space spanned by the principal portfolios with the smallest $S - C$ eigenvalues. Then, we define the spectral residual as

$$\tilde{\epsilon} = \mathbf{A}_{\text{res}} \mathbf{r}. \quad (8)$$

B.1 Isotropic residuals

First, we prove the following result, which corresponds to Proposition 1 in the main body.

Proposition 2 (Proposition 1 in the main body, restated). Let \mathbf{r} be a random vector in \mathbb{R}^S generated according to a linear model $\mathbf{r} = \mathbf{B}\mathbf{f} + \epsilon$, where \mathbf{B} is an $S \times C$ matrix of full column rank, and $\mathbf{f} \in \mathbb{R}^C$ and $\epsilon \in \mathbb{R}^S$ are zero-mean random vectors. Assume that the following conditions hold:

- $\text{Var}(f_i) = 1$ and $\text{Var}(\epsilon_k) = \sigma > 0$.
- The coordinate variables in \mathbf{f} and ϵ are uncorrelated, that is, $\mathbb{E}[f_i f_j] = 0$, $\mathbb{E}[\epsilon_k \epsilon_\ell] = 0$, and $\mathbb{E}[f_i \epsilon_k] = 0$ hold for any $i \neq j$ and $k \neq \ell$.

Then, we have the followings.

- (i) The spectral residual $\tilde{\epsilon}$ defined in (8) is uncorrelated from the common factor \mathbf{f} .
- (ii) The covariance matrix of $\tilde{\epsilon}$ is given as $\sigma^2 \mathbf{A}_{\text{res}}$. Under a suitable assumption, this can be approximated as a diagonal matrix.

Proof. Let $\mathbf{B}\mathbf{B}^\top = \mathbf{V}_{\text{mar}} \mathbf{\Lambda} \mathbf{V}_{\text{mar}}^\top$ be the eigendecomposition of the market factor covariance $\mathbf{B}\mathbf{B}^\top$, where $\mathbf{V}_{\text{mar}} = [\mathbf{v}_1, \dots, \mathbf{v}_S]$ is an orthogonal matrix and $\mathbf{\Lambda}$ is a diagonal matrix of the eigenvalues. Since $\text{rank} \mathbf{B}\mathbf{B}^\top \leq C$, we can write

$$\mathbf{\Lambda} = \text{diag}(\lambda_1, \dots, \lambda_C, \underbrace{0, \dots, 0}_{S-C}).$$

Note that $\lambda_i > 0$ for all $i \in \{1, \dots, C\}$ since $\mathbf{B}\mathbf{B}^\top$ is positively semi-definite and has rank C . Since coordinate

⁴In general, \mathbf{V}_{res} is not unique because there can be multiple eigenvectors having the same eigenvalues. For simplicity, we assume that $\lambda_C > \lambda_{C+1}$ so that \mathbf{V}_{res} is uniquely determined.

variables in \mathbf{f} and ϵ are uncorrelated, the covariance matrix of \mathbf{r} is calculated as

$$\Sigma = \mathbf{B}\mathbf{B}^\top + \sigma^2 \mathbf{I} = \mathbf{V}_{\text{mar}}(\Lambda + \sigma^2 \mathbf{I})\mathbf{V}_{\text{mar}}^\top.$$

This gives the eigendecomposition of Σ , and its eigenvalues are given as

$$\underbrace{\lambda_1 + \sigma^2, \dots, \lambda_C + \sigma^2}_C, \underbrace{\sigma^2, \dots, \sigma^2}_{S-C}.$$

In particular, the projection matrix for the spectral residual is given as

$$\mathbf{A}_{\text{res}} = [\mathbf{v}_{C+1}, \dots, \mathbf{v}_S][\mathbf{v}_{C+1}, \dots, \mathbf{v}_S]^\top. \quad (9)$$

Consequently, we have $\tilde{\epsilon} = \mathbf{A}_{\text{res}}(\mathbf{B}\mathbf{f} + \epsilon) = \mathbf{A}_{\text{res}}\epsilon$, which is uncorrelated from $\mathbf{B}\mathbf{f}$ (thus we proved (i)).

Moreover, the covariance matrix of $\mathbf{A}_{\text{res}}\epsilon$ is given as $\sigma^2 \mathbf{A}_{\text{res}}\mathbf{A}_{\text{res}}^\top = \sigma^2 \mathbf{A}_{\text{res}}$. Regarding the diagonal approximation of this matrix, see the next subsection for details. \square

B.2 On the near-orthogonality of spectral residuals

When we construct a portfolio over the spectral residuals, we use an diagonal approximation of the covariance matrix (see Section 3.2 and Appendix A.1). As mentioned in the previous subsection, this covariance matrix is proportional to \mathbf{A}_{res} . Hence, to justify the diagonal approximation, we should show that \mathbf{A}_{res} becomes nearly diagonal.

Figure 6 shows examples of \mathbf{A}_{res} calculated empirically from U.S. market data. For several choices of the parameter C , these matrices are reasonably close to diagonal matrices.

But why does this happen? Generally speaking, a projection matrix constructed as (9) is not necessarily approximated well by a diagonal matrix. However, in financial markets, we may assume that the following properties hold for the first several principal portfolios, which may justify the diagonal approximation.

- **Well-spreading factors:** In a financial market, a large proportion of a stock return is often explained by a small number of common market factors. A market factor may be almost equally shared by all the stocks in the market. For example, the first principal portfolio can be seen as the factor of the overall market, which may be close to the “equal weighting index” of stocks. In this case, removing the market factor changes all the elements of the covariance matrix only very slightly.
- **Spiked factors:** Suppose that, in an investment horizon, a certain company’s stock price is affected by a factor that is independent from any other market factors. In this situation, there can be a principal portfolio that arises only from a single stock. Removing this factor is just equivalent to removing the corresponding stock, which does not affect the off-diagonal elements of the covariance matrix.

To formulate the above idea, we introduce the following two notions.

Definition 3. Let $\mathbf{v} \in \mathbb{R}^S$ be a unit vector (i.e., $\|\mathbf{v}\|_2 = 1$). Let $\delta > 0$ be a positive number.

- We say that \mathbf{v} is δ -spreading if $|v_i| \leq \sqrt{\delta/S}$ for all $i \in \{1, \dots, S\}$.
- We say that \mathbf{v} is δ -spiked if there exists $i^* \in \{1, \dots, S\}$ such that $|v_i| \leq \delta/S$ for all $i \neq i^*$.

The above properties ensure that the off-diagonal elements of $\mathbf{v}\mathbf{v}^\top$ are sufficiently small.

Proposition 3. Suppose that a unit vector $\mathbf{v} \in \mathbb{R}^S$ is either δ -spreading or δ -spiked for some $\delta > 0$. Then, for all $i \neq j$, the (i, j) element of $\mathbf{P} = \mathbf{v}\mathbf{v}^\top$ is bounded as $|P_{ij}| = |v_i v_j| \leq \delta/S$.

Proof. The conclusion is obvious if \mathbf{v} is δ -spreading. If \mathbf{v} is δ -spiked, we have $|v_i v_j| \leq 1 \cdot \delta/S = \delta/S$ for any $i \neq j$. \square

Now, let us consider the linear factor model $\mathbf{r} = \mathbf{B}\mathbf{f} + \epsilon$. We assume a similar condition as in Proposition 2. In particular, we assume that ϵ has an isotropic covariance matrix $\sigma^2 \mathbf{I}$. Our goal is to show that the spectral residual $\mathbf{A}_{\text{res}}\mathbf{r}$ has a nearly isotropic covariance matrix under a suitable condition.

Let $\mathbf{B}\mathbf{B}^\top = \mathbf{V}_{\text{mar}}\Lambda\mathbf{V}_{\text{mar}}^\top$ be an eigendecomposition of the market factor, where \mathbf{V} is an orthogonal matrix and $\Lambda = \text{diag}(\lambda_1, \dots, \lambda_C, 0, \dots, 0)$ with $\lambda_1 \geq \dots \geq \lambda_C > 0$. Then, as in Proposition 2, we have

$$\begin{aligned} \mathbf{A}_{\text{res}} &= [\mathbf{v}_{C+1}, \dots, \mathbf{v}_S][\mathbf{v}_{C+1}, \dots, \mathbf{v}_S]^\top \\ &= \mathbf{I} - \mathbf{P}_{\text{mar}}, \end{aligned}$$

and the spectral residual is given as $\mathbf{A}_{\text{res}}\mathbf{r} = \mathbf{A}_{\text{res}}\epsilon$. Here,

$$\mathbf{P}_{\text{mar}} = [\mathbf{v}_1, \dots, \mathbf{v}_C][\mathbf{v}_1, \dots, \mathbf{v}_C]^\top$$

is the projection matrix onto the space of the market factors. Thus, the covariance matrix of the spectral residual is given as $\sigma^2 \mathbf{A}_{\text{res}}$. The following proposition explains that this covariance matrix is nearly diagonal if the top- C principal portfolios are either “well-spreading” or “nearly spiked”.

Proposition 4. We use similar notations and assumptions as above. Suppose that each \mathbf{v}_i ($i \in \{1, \dots, C\}$) is either δ -spreading or δ -spiked. Then, the off-diagonal elements of \mathbf{A}_{res} are bounded as

$$|[\mathbf{A}_{\text{res}}]_{i,j}| \leq \frac{C\delta}{S}$$

for any $i \neq j$.

Proof. Combining the equality $\mathbf{P}_{\text{mar}} = \sum_{i=1}^C \mathbf{v}_i \mathbf{v}_i^\top$ and the fact that all the absolute values of the off-diagonal elements in $\mathbf{v}_i \mathbf{v}_i^\top$ are not larger than δ/S , we have $|[\mathbf{A}_{\text{res}}]_{i,j}| = |[\mathbf{P}_{\text{mar}}]_{i,j}| \leq C\delta/S$ for any $i \neq j$. Hence the result. \square

B.3 Anisotropic residuals

Proposition 2 does not hold when the true residual factor $\epsilon_1, \dots, \epsilon_S$ are anisotropic. However, we can show that the spectral residual is almost uncorrelated from the market factors if

- the volatilities of market factors are sufficiently larger than the residual factors, and
- the residual factors are almost isotropic.

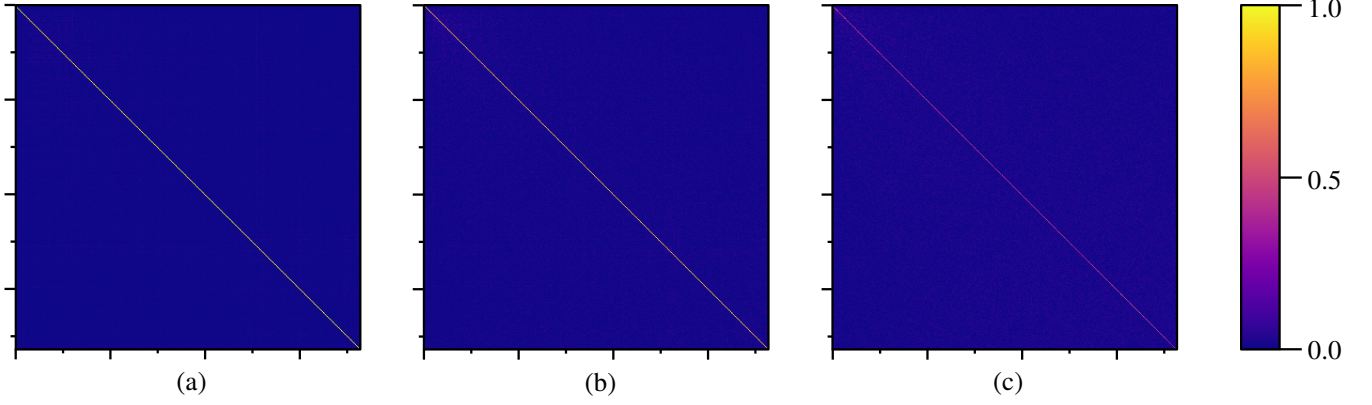


Figure 6: The absolute values of projection matrix \mathbf{A}_{res} calculated from U.S. market data. Three panels show results for (a) $C = 10$, (b) $C = 50$, and (c) $C = 200$, respectively. In all cases, the projection matrices are reasonably close to diagonal matrices.

Here, we provide a quantitative justification of this claim by using matrix perturbation theory (Davis and Kahan 1970; Yu, Wang, and Samworth 2014).

Before describing the result, we provide some notations. For any $S \times S$ matrix \mathbf{A} , $\|\mathbf{A}\|_{\text{F}}$ is the Frobenius norm defined as $\|\mathbf{A}\|_{\text{F}}^2 = \sum_{i,j} a_{ij}^2$. For any orthogonal projection matrix \mathbf{P} , let $\mathcal{V}(\mathbf{P})$ denote the corresponding linear subspace (i.e., the largest linear subspace that is invariant under \mathbf{P}). Let \mathbf{P}_1 and \mathbf{P}_2 be any two orthogonal projection matrices having the same rank, and $\mathcal{V}_i = \mathcal{V}(\mathbf{P}_i)$ ($i = 1, 2$). Then, the quantity

$$\|\sin \Theta(\mathcal{V}_1, \mathcal{V}_2)\|_{\text{F}} := \|\mathbf{P}_1(\mathbf{I} - \mathbf{P}_2)\|_{\text{F}} = \|\mathbf{P}_2(\mathbf{I} - \mathbf{P}_1)\|_{\text{F}}$$

measures the ‘‘principal angles’’ between two subspaces \mathcal{V}_1 and \mathcal{V}_2 (Davis and Kahan 1970). In particular, this quantity becomes zero if and only if the two subspaces agree.

Proposition 5. Let \mathbf{r} be a random vector in \mathbb{R}^S generated according to a linear model $\mathbf{r} = \mathbf{B}\mathbf{f} + \boldsymbol{\epsilon}$, where \mathbf{B} is an $S \times C$ matrix of full rank, and $\mathbf{f} \in \mathbb{R}^C$ and $\boldsymbol{\epsilon} \in \mathbb{R}^S$ are zero-mean random vectors. Assume that the following conditions hold:

- $\text{Var}(f_i) = 1$ and $\text{Var}(\epsilon_k) = \sigma_k^2 > 0$ for $k \in \{1, \dots, S\}$.
- The coordinate variables in \mathbf{f} and $\boldsymbol{\epsilon}$ are uncorrelated, that is, $\mathbb{E}[f_i f_j] = 0$, $\mathbb{E}[\epsilon_k \epsilon_\ell] = 0$, and $\mathbb{E}[f_i \epsilon_k] = 0$ hold for any $i \neq j$ and $k \neq \ell$.

Let \mathbf{P}_{mar} be the orthogonal projection matrix onto the linear space spanned by \mathbf{B} , and let \mathbf{A}_{res} be the projection matrix of the spectral residuals. Let λ_{\min} be the smallest positive eigenvalue of $\mathbf{B}\mathbf{B}^\top$. Then, we have

$$\|\mathbf{P}_{\text{mar}}\mathbf{A}_{\text{res}}\|_{\text{F}} \leq \frac{2\sqrt{S}(\max_i \sigma_i^2 - \min_i \sigma_i^2)}{\lambda_{\min}}. \quad (10)$$

Here, we give an interpretation of (10). If $\|\mathbf{P}_{\text{mar}}\mathbf{A}_{\text{res}}\|_{\text{F}}$ is shown to be small, the spectral residual $\mathbf{A}_{\text{res}}\mathbf{r}$ is nearly orthogonal to any market factors. The right-hand side of (10) can be small when either of the following conditions are satisfied: (i) If the residual factors are nearly isotropic, then $\max_i \sigma_i^2 - \min_i \sigma_i^2$ is small. (ii) If the smallest variance of the market factor λ_{\min} is much larger than $\sqrt{S}(\max_i \sigma_i^2 - \min_i \sigma_i^2)$, the right-hand side becomes small.

Proof. Since \mathbf{f} and $\boldsymbol{\epsilon}$ are uncorrelated, the covariance matrix of the generative model $\mathbf{r} = \mathbf{B}\mathbf{f} + \boldsymbol{\epsilon}$ can be written as $\boldsymbol{\Sigma} = \mathbf{B}\mathbf{B}^\top + \mathbf{Q}$, where $\mathbf{Q} = \text{diag}(\sigma_1^2, \dots, \sigma_S^2)$ is the variance of the residual factors.

Let $\bar{s} = \frac{1}{S} \sum_{i=1}^S \sigma_i^2$ be the averaged variance of the residual factors. As such, $\bar{s}\mathbf{I}$ is the closest isotropic covariance matrix of \mathbf{Q} in the following sense:

$$\bar{s}\mathbf{I} \in \underset{s\mathbf{I}: s \geq 0}{\text{argmin}} \|\mathbf{Q} - s\mathbf{I}\|_{\text{F}}.$$

Let $\hat{\mathbf{Q}} = \bar{s}\mathbf{I} - \mathbf{Q}$. Define $\Delta_{\text{iso}} \geq 0$ as

$$\Delta_{\text{iso}} := \|\hat{\mathbf{Q}}\|_{\text{F}} = \min_{s\mathbf{I}: s \geq 0} \|\mathbf{Q} - s\mathbf{I}\|_{\text{F}} = \left(\sum_{i=1}^S (\sigma_i^2 - \bar{s})^2 \right)^{1/2},$$

which quantifies how far \mathbf{Q} is away from being isotropic.

As in the proof of Proposition 2, let $\mathbf{B}\mathbf{B}^\top = \mathbf{V}_{\text{mar}}\boldsymbol{\Lambda}\mathbf{V}_{\text{mar}}^\top$ be the eigendecomposition of $\mathbf{B}\mathbf{B}^\top$. Define $\hat{\boldsymbol{\Sigma}}$ as

$$\hat{\boldsymbol{\Sigma}} = \boldsymbol{\Sigma} + \hat{\mathbf{Q}} = \mathbf{B}\mathbf{B}^\top + \bar{s}\mathbf{I}.$$

Since $\mathbf{B}\mathbf{B}^\top$ and $\bar{s}\mathbf{I}$ are simultaneously diagonalizable by \mathbf{V}_{mar} , we can write

$$\hat{\boldsymbol{\Sigma}} = \mathbf{V}_{\text{mar}}(\boldsymbol{\Lambda} + \bar{s}\mathbf{I})\mathbf{V}_{\text{mar}}^\top.$$

In particular, the eigenvalues of $\hat{\boldsymbol{\Sigma}}$ are given as

$$\underbrace{\lambda_1 + \bar{s}, \dots, \lambda_C + \bar{s}}_C, \underbrace{\bar{s}, \dots, \bar{s}}_{S-C}.$$

Let \mathbf{P}_{mar} be the orthogonal projection matrix onto the linear subspace spanned by the column vectors of \mathbf{B} (i.e., the market factors). Note that such a linear subspace is spanned by $\mathbf{v}_1, \dots, \mathbf{v}_C$, and \mathbf{P}_{mar} is computed as

$$\mathbf{P}_{\text{mar}} = [\mathbf{v}_1, \dots, \mathbf{v}_C][\mathbf{v}_1, \dots, \mathbf{v}_C]^\top.$$

Also, let $\boldsymbol{\Sigma} = \mathbf{U}\mathbf{M}\mathbf{U}^\top$ be the eigendecomposition of $\boldsymbol{\Sigma}$, where $\mathbf{U} = [\mathbf{u}_1, \dots, \mathbf{u}_S]$ is an orthogonal matrix, and $\mathbf{M} = \text{diag}(\mu_1, \dots, \mu_S)$ is a diagonal matrix with $\mu_1 \geq$

$\dots \geq \mu_C > \mu_{C+1} \geq \dots \mu_S > 0$ ⁵. Then, the projection matrix for the spectral residual is given as

$$\mathbf{A}_{\text{res}} = [\mathbf{u}_{C+1}, \dots, \mathbf{u}_S][\mathbf{u}_{C+1}, \dots, \mathbf{u}_S]^\top.$$

Now, \mathbf{P}_{mar} and $\mathbf{I} - \mathbf{A}_{\text{res}}$ are the projection matrices that correspond to eigenvectors with the largest C eigenvalues of $\widehat{\Sigma}$ and Σ , respectively. From Davis–Kahan $\sin \theta$ theorem (Davis and Kahan 1970; Yu, Wang, and Samworth 2014), we conclude

$$\|\mathbf{P}_{\text{mar}}\mathbf{A}_{\text{res}}\|_{\text{F}} \leq \frac{2\|\widehat{\Sigma} - \Sigma\|_{\text{F}}}{\min_{1 \leq i \leq C} \lambda_i} = \frac{2\Delta_{\text{iso}}}{\min_{1 \leq i \leq C} \lambda_i}.$$

We also have a weaker inequality (10) since $\Delta_{\text{iso}} \leq \sqrt{S}(\max_i \sigma_i^2 - \min_i \sigma_i^2)$. \square

C Details for experimental settings

In this section, we provide some more details on the experiments in Section 4.

C.1 Definitions of additional evaluation metrics

- *Maximum DrawDown (MDD)* is the maximum loss from a peak to a trough (Grossman and Zhou 1993), which can measure one aspect of downside risk:

$$\text{MDD}_T = \max_{t \in \{1, \dots, T\}} \max_{s \in \{1, \dots, t\}} \left(\frac{\text{CW}_t - \text{CW}_s}{\text{CW}_t} \right). \quad (11)$$

- *Calmar Ratio (CR)* is a risk-adjusted return based on the maximum drawdown (Young 1991): $\text{CR}_T := \text{AR}_T / \text{MDD}_T$.
- *Downside Deviation Ratio (DDR)* (a.k.a. Sortino Ratio) is a variation of the Sharpe ratio (Sortino and Price 1994). While the Sharpe ratio regards overall volatility as risk, it regards only volatility caused by negative returns as harmful risk:

$$\text{DDR}_T := \frac{\text{AR}_T}{\sqrt{\frac{T_Y}{T} \sum_{i=1}^T \min(0, R_t)^2}}. \quad (12)$$

C.2 Definitions of some baseline methods

- **Reversal strategy.** In Section 4.2 and Section 4.3, we used a simple reversal strategy ($\text{AR}(1)$) as a benchmark method, which is defined as follows. Let \mathbf{r}_t ($t = 1, 2, \dots$) be either a return sequence or a transformed return sequence (e.g., the spectral residuals). Then, the reversal strategy \mathbf{b}_t is defined by renormalizing $-\mathbf{r}_{t-1}$ to be a zero-investment portfolio, that is,

$$\mathbf{b}_t = \frac{\mathbf{r}_{t-1} - \bar{r}_{t-1}\mathbf{1}}{\|\mathbf{r}_{t-1} - \bar{r}_{t-1}\mathbf{1}\|_1},$$

where $\bar{r}_{t-1} = \frac{1}{S} \sum_{i=1}^S r_{t-1}$.

⁵This is true for many cases where the market factors are much larger than the residual factors. For example, let $\delta = \|\widehat{\mathbf{Q}}\|_{\text{op}} = \max_j |\sigma_j^2 - \bar{s}|$, and suppose that $\lambda_C = \min_i \lambda_i > 2\delta$. Then, from the well-known Weyl’s inequality on eigenvalues, we have $\mu_C \geq \lambda_C + \bar{s} - \delta > \bar{s} + \delta \geq \mu_{C+1}$.

- **MLP-based prediction.** In Section 4.2, we also used a neural network-based prediction of returns (MLP). We used a fully-connected neural network with 4 hidden layers. Each hidden layer has 512 nodes, 50% dropout and batch normalization.

C.3 Details of network architectures and hyperparameters

Here, we explain the details of the architecture that we used for the distributional prediction. For each coordinate $i \in \{1, \dots, S\}$ of the spectral residual, we applied a common non-linear function $\psi : \mathbb{R}^H \rightarrow \mathbb{R}^{Q-1}$ that predicts $Q - 1$ quantiles based on the past H observations. We designed ψ by the fractal network introduced in Section 3.3. The detailed specifications are as follows.

- We estimate $Q - 1 = 31$ quantiles for each stock. In particular, j -th coordinate of ψ corresponds to the $\frac{j}{32}$ -th quantile of the future distribution.
- The resampling mechanism $\text{Resample}(\mathbf{x}, \tau)$ outputs sequences of a fixed length $H' = 64$. For the scale parameters, we used $\tau_j := 4^{-j/20}$ with $j \in \{0, \dots, 21\}$.
- For the function $\psi_1 : \mathbb{R}^{H'} \rightarrow \mathbb{R}^K$ (with $K = 256$), we used a fully connected neural network with 3 hidden layers. Each layer has 256 nodes, 50% dropout and batch normalization.
- For the function $\psi_2 : \mathbb{R}^K \rightarrow \mathbb{R}^{Q-1}$, we used a fully connected neural network with 8 hidden layers. Each layer has 128 nodes, 50% dropout and batch normalization.
- For training, we used the Adam optimizer (Kingma and Ba 2015) with learning rate 0.001.

D Supplementary experiments for spectral residuals

In this section, we provide additional experimental results on the spectral residual. In Section D.1, we conduct a simple experiment to show that the short-term behavior of the (empirical) spectral residual is reasonably stable. In Section D.2, we discuss a simple way to determine the parameter C from the training data.

D.1 Local stability of spectral residuals

We check whether the spectral residuals are locally stable. This is not trivial because (i) the spectral residual is calculated locally on time windows, and (ii) the long-term behavior of the financial time series is highly non-stationary. To this end, we here investigate the ability of the spectral residuals to reduce the volatility of sequences.

For each time t , we calculated the projection matrix (\mathbf{A}_t defined in Section 3.1) and the spectral residuals $\tilde{\epsilon}_s$ for $t - H \leq s \leq t - 1$. We also generated the spectral residuals for unseen duration $t \leq s < t + H$ by fixing \mathbf{A}_t and extrapolating the relation $\tilde{\epsilon}_s = \mathbf{A}_t \mathbf{r}_s$. Then, we calculated the volatility $\text{Vol}(\tilde{\epsilon}_s)$ of the spectral residual at each s . Throughout, we fixed $H = 256$, and we varied the number of principal components to be removed as $C \in \{0, 1, 10, 20, 50, 100\}$.

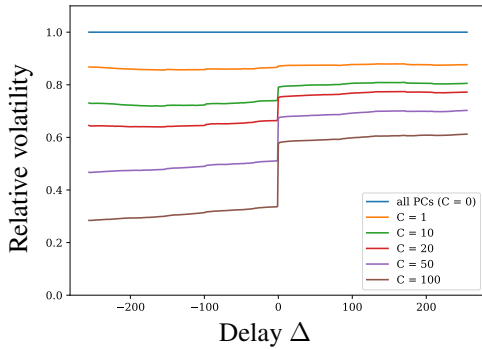


Figure 7: Relative volatility to the raw stock returns for various choices of parameter C . The ability to reduce the volatility seems to continue in the unseen duration ($\Delta > 0$), which may suggest the local stability of spectral residuals. See the text for details.

Table 3: Performance comparison of reversal returns on different numbers of principal components (PCs) to be eliminated (U.S. market).

	ASR \uparrow	AR \uparrow	AVOL \downarrow	DDR \uparrow	CR \uparrow	MDD \downarrow
$C = 0$	+0.759	+0.076	0.058	+1.325	+0.367	0.158
$C = 1$	+0.753	+0.054	0.041	+1.343	+0.309	0.132
$C = 10$	+1.426	+0.035	0.049	+2.541	+1.206	0.041
$C = 20$	+1.317	+0.028	0.037	+2.288	+1.000	0.037
$C = 50$	+1.264	+0.019	0.024	+2.275	+0.990	0.025
$C = 100$	+1.089	+0.013	0.014	+1.877	+0.391	0.035

Figure 7 shows the result averaged over t , which illustrates the proportion of the volatility of spectral residuals ($C \geq 1$) to the volatility of raw stock returns ($C = 0$). The horizontal axis is the delay parameter $\Delta := s - t \in \{-H, \dots, 0, \dots, H - 1\}$. Here, $\Delta < 0$ corresponds to the “observed” duration used for calculating the projection matrix A_t , and $\Delta \geq 0$ corresponds to the “unseen” duration generated by extrapolation. From this, we observe the followings:

- **Monotonicity.** Increasing the number C of eliminated principal components can reduce the volatility of the spectral residuals even for the unseen duration.
- **Local stability.** Regarding the volatility proportion, the difference between the observed duration and the unseen duration increases with increasing C . Remarkably, the first principal component (a.k.a. the market factor) is quite stable, and the volatility proportion for $C = 1$ is well extrapolated to the unseen duration.

The above observations suggest that the projection matrix A_t can be locally stable if C is not too large. Hence, we can extract meaningful residual information in the subsequent time window by extrapolating the projection matrix.

D.2 Choosing the number of eliminated factors

Next, we consider the appropriate choice of the parameter C to make trading strategies robustly profitable. Figure 8 and

Table 4: Performance comparison of reversal returns on different numbers of principal components (PCs) to be eliminated (Japanese market).

	ASR \uparrow	AR \uparrow	AVOL \downarrow	DDR \uparrow	CR \uparrow	MDD \downarrow
$C = 0$	+1.259	+0.082	0.065	+2.344	+0.700	0.117
$C = 1$	+1.715	+0.087	0.050	+3.169	+1.103	0.078
$C = 10$	+2.960	+0.074	0.025	+5.555	+2.037	0.036
$C = 20$	+3.291	+0.071	0.022	+6.306	+4.215	0.017
$C = 50$	+3.036	+0.047	0.016	+5.938	+3.258	0.015
$C = 100$	+2.175	+0.023	0.011	+4.114	+1.152	0.020

Table 5: Performance comparison on the Japanese market.

	ASR \uparrow	AR \uparrow	AVOL \downarrow	DDR \uparrow	CR \uparrow	MDD \downarrow
Market	+0.819	+0.158	0.193	+1.320	+0.636	0.248
AR(1)	+1.511	+0.058	0.038	+2.684	+1.094	0.053
AR(1) on SRes	+1.835	+0.034	0.019	+3.237	+1.112	0.031
Linear on SRes	+1.380	+0.023	0.017	+2.469	+0.952	0.024
MLP on SRes	+1.802	+0.030	0.017	+3.280	+0.963	0.032
SFM on SRes	+0.250	+0.005	0.019	+0.442	+0.116	0.042
DPO-NQ	+1.369	+0.024	0.018	+2.379	+0.758	0.032
DPO-NF	+1.770	+0.030	0.017	+3.159	+1.165	0.025
DPO-NV	+1.979	+0.039	0.020	+3.516	+1.484	0.026
DPO	+2.171	+0.036	0.017	+3.878	+1.460	0.025

Table 3 show the performance of the reversal strategy over the spectral residuals on U.S. market.

From the result, we observe the followings. With increasing the number C of eliminated principal components, both AR and AVOL tend to decrease. This is because eliminating more principal components reduces the volatility, while it becomes more difficult to earn large returns from the remaining information. Especially, eliminating the first 10 principal components ($C = 10$) attained the best trade-off between the return and the risk, and thus had the best ASR value.

We also conducted a similar experiment on Japanese market data, in which $C = 20$ achieved the best ASR value. See Figure 9 and Table 4 for corresponding results.

E Performance evaluation on Japanese market data

Here, we evaluated the performance of our proposed system (DPO) on Japanese market data. We used similar evaluation metrics and baseline methods presented in Section 4.3.

E.1 Japanese market data

For Japanese market data, we used daily prices of stocks listed in TOPIX 500 from January 2005 to December 2018. We used data before January 2012 for training and validation and the remainder for testing. We obtained the data from Japan Exchange Group (JPX)⁶.

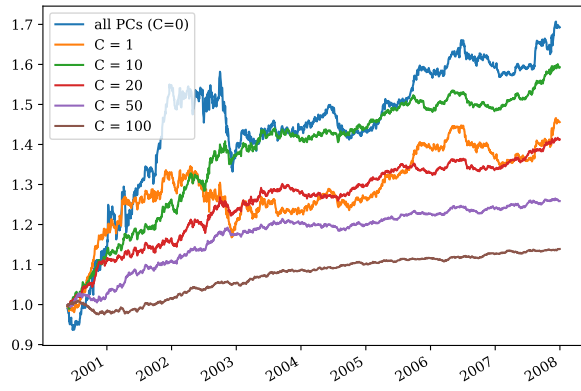


Figure 8: The Cumulative Wealth of the reversal strategy with different choices of the number C of principal components to be eliminated (U.S. market).

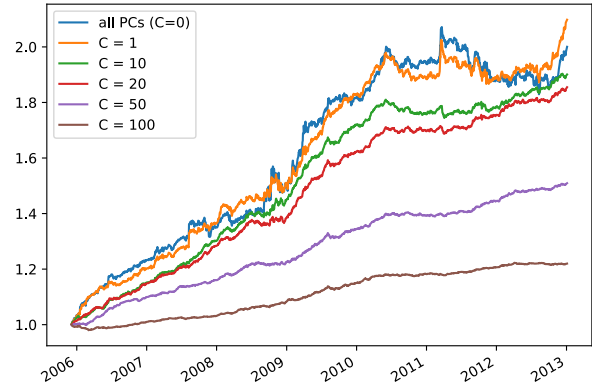


Figure 9: The Cumulative Wealth of the reversal strategy with different choices of the number C of principal components to be eliminated (Japanese market).

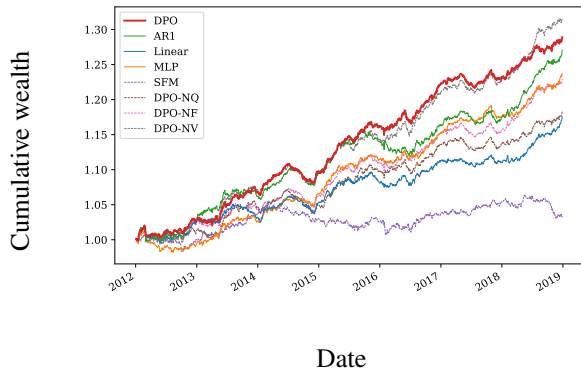


Figure 10: The Cumulative Wealth in Japanese market.

E.2 Results

Table 5 and Figure 10 show the results. Overall, we obtained consistent results with those on U.S. market. Our proposed method (DPO) outperformed other baseline methods and ablation models in the ASR. For other evaluation metrics, DPO achieved comparable performance to the best performing baselines.

⁶<https://www.jpx.co.jp/english/markets/>